

# Complex shape evolution of electromigration-driven single-layer islands

Philipp Kuhn,<sup>1,2</sup> Joachim Krug,<sup>2,\*</sup> Frank Hausser,<sup>3</sup> and Axel Voigt<sup>3</sup>

<sup>1</sup>*Fachbereich Physik, Universität Duisburg-Essen, 45117 Essen, Germany*

<sup>2</sup>*Institut für Theoretische Physik, Universität zu Köln, Zùlpicher Strasse 77, 50937 Köln, Germany*

<sup>3</sup>*Crystal Growth group, research center caesar, Ludwig-Erhard-Allee 3, 53175 Bonn, Germany*

(Dated: October 28, 2004)

The shape evolution of two-dimensional islands through periphery diffusion biased by an electromigration force is studied numerically using a continuum approach. We show that the introduction of crystal anisotropy in the mobility of edge atoms induces a rich variety of migration modes, which include oscillatory and irregular behavior. A phase diagram in the plane of anisotropy strength and island size is constructed. The oscillatory motion can be understood in terms of stable facets which develop on one side of the island and which the island then slides past. The facet orientations are determined analytically.

PACS numbers: 68.65.-k, 66.30.Qa, 05.45.-a, 85.40.-e

The nucleation, growth, diffusion and shape evolution of single layer islands on a crystalline surface has been the focus of much recent research activity [1]. Apart from their importance as templates for the growth of multilayer films and heterostructures, arrays of two-dimensional islands provide a convenient framework in which our understanding of nanostructure evolution, from atomistic to mesoscopic scales, can be confronted with detailed experimental observations using scanning probe techniques.

In this Letter we report the discovery of a remarkable richness of dynamical behaviors displayed by single layer islands under the influence of surface electromigration, the directed motion of adsorbed atoms due to the slight force transmitted by collisions with conduction electrons on the surface of a current carrying sample. It has been appreciated for some time now that electromigration is able to induce dramatic morphological changes on crystal surfaces, the most well-studied manifestation being the bewildering variety of step patterns observed on surfaces vicinal to Si(111) [2]. The electromigration-driven motion of single layer islands has been studied experimentally by reflection electron microscopy on Si(111) [3, 4], and theoretically using Monte Carlo simulations [5] as well as continuum theory [6].

The continuum approach to island shape evolution, which treats the island edge as a curve endowed with a (generally anisotropic) line tension, has been successfully applied to a range of problems including the diffusion [7] and sintering [8] of islands, and the pinch-off of vacancy clusters [9]. Here we focus on the regime of periphery diffusion (PD), where the dominant kinetic process is the migration of atoms along the island boundary. The shape then follows a local evolution law, without coupling to the adatom concentration on the surrounding terrace. We extend the model of [6] by including crystal anisotropy in the adatom mobility. This turns out to have far-reaching consequences: In addition to the scenarios of steady motion and island breakup [6, 10, 11] observed in previous

work, we find a variety of new dynamic phenomena including spontaneous symmetry breaking in the direction of island motion, oscillatory shape evolution, and complex migration trajectories where different modes of motion alternate in a periodic or irregular fashion.

Oscillatory shape changes were found previously in a nonlocal model of void electromigration in metallic thin films [12], and spontaneous symmetry breaking as well as periodic, quasiperiodic and chaotic behavior has been seen in theoretical studies of directional solidification [13, 14]. To the best of our knowledge, however, our work provides the first example of complex shape evolution for a *closed* contour subject to purely *local* dynamics.

In the PD regime, the normal velocity  $v_n$  of the island boundary satisfies the continuity equation

$$v_n + \frac{\partial}{\partial s} \Omega \sigma \left[ -\frac{\partial}{\partial s} (\Omega \tilde{\gamma} \kappa) + q^* E_t \right] = 0. \quad (1)$$

Here  $s$  denotes the arclength along the island edge, and  $\Omega$  the atomic area. The square bracket multiplied by the edge atom mobility  $\sigma$  is the total mass current along the boundary, which is driven by the tangential derivative of the chemical potential [1]  $\Delta \mu = \Omega \tilde{\gamma} \kappa$  and the electromigration force  $q^* E_t$ ;  $\tilde{\gamma}$  is the edge stiffness,  $\kappa$  the local curvature,  $q^*$  the effective charge of an edge atom, and  $E_t$  the tangential component of the local electric field. The crystal anisotropy of the surface enters through the dependence of  $\tilde{\gamma}$  [15] and  $\sigma$  [8, 16] on the orientation angle  $\theta$  of the island edge.

For atomic layer height islands on the surface of a thick sample, the island boundary has a negligible effect on the electric field; this is in contrast to the modeling of insulating voids in macroscopic metallic thin films, where the coupling of the void shape to the electric field leads to a manifestly nonlocal problem [10, 11, 12]. Here we can take the field to be of constant strength  $E_0$  and aligned along the  $x$ -axis. Letting  $\theta$  denote the angle between the normal of the island edge and the  $y$ -axis (counted positive in the clockwise direction), this implies  $E_t = E_0 \cos(\theta)$ .

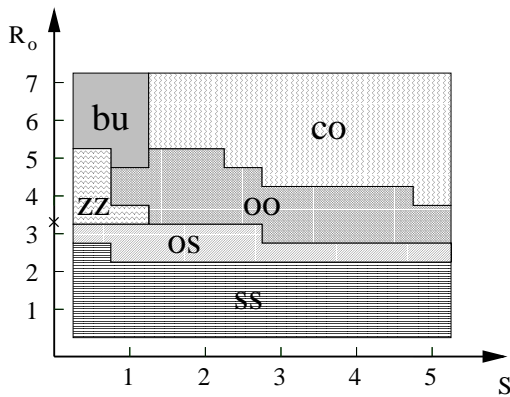


FIG. 1: Phase diagram of migration modes in the plane of anisotropy strength  $S$  and island radius  $R_0$ , for sixfold anisotropy ( $n = 6$ ) and the field aligned with a direction of maximal mobility ( $\alpha = 0$ ). For each point on a grid of resolution  $0.5 \times 0.5$ , the evolution of the island was followed until the asymptotic mode could be identified. We distinguish between straight stationary (**ss**), oblique stationary (**os**), oblique oscillatory (**oo**), zigzag (**zz**) and complex oscillatory (**co**) motion. In the region **bu** islands break up. The cross on the  $R_0$ -axis indicates the linear instability of the circular solution in the isotropic case.

Together with the specification of  $\tilde{\gamma}$  and  $\sigma$ , to be addressed below, this completes the definition of the local boundary evolution (1). Comparing the two terms inside the square brackets, we extract the characteristic length scale [6, 11, 17]  $l_E = \sqrt{\Omega \tilde{\gamma} / |q^* E_0|}$ , which gauges the relative importance of capillary and electromigration forces; electromigration dominates on scales large compared to  $l_E$ . Below all lengths are reported in units of  $l_E$ .

The isotropic version of (1), with  $\tilde{\gamma}, \sigma = \text{const.}$ , has been studied previously by Suo and collaborators [17, 18, 19]. A circular island moving at constant velocity is stable for (dimensionless) radii  $R < R_c \approx 3.26$  [19]. Beyond the instability a bifurcation to two branches of non-circular stationary solutions occurs [18]. Numerical integration of the time-dependent problem [20] shows that only one of the branches, corresponding to islands elongated in the field direction, is realized. At large radii island breakup occurs, mediated by the outgrowth of a finger of the kind found in [17].

We now turn to the effects of crystal anisotropy. Throughout this paper only the anisotropy of the adatom mobility  $\sigma$  will be taken into account, while the edge stiffness  $\tilde{\gamma}$  is kept isotropic. This is motivated partly by the fact that the anisotropy in  $\sigma$  is found experimentally (to the extent that it has been investigated) to much exceed that of  $\tilde{\gamma}$  [16], and partly by our desire to disentangle kinetic ( $\sigma$ ) and thermodynamic ( $\tilde{\gamma}$ ) effects [21]. For the kinetic anisotropy we employ the functional form [11]

$$\sigma(\theta) = \sigma_{\max}(1 + S)^{-1} \{1 + S \cos^2[n(\theta + \alpha)/2]\}. \quad (2)$$

Since the prefactor  $\sigma_{\max}$  only sets the time scale, the

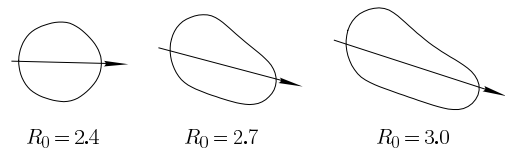


FIG. 2: Stationary shapes for  $S = 2$  near the transition from **ss** to **os** behavior. Arrows indicate the direction of motion.

relevant parameters in (2) are the anisotropy strength  $S$ , the number of symmetry axes  $n$ , and the angle  $\alpha$  between the symmetry axes and the electric field direction. The natural time unit is  $t_E = l_E^4 / (\sigma_{\max} \tilde{\gamma} \Omega^2)$  [11].

The simplest solutions in the anisotropic case are stationary islands moving at constant speed, which satisfy the equation  $v_n = V \sin(\theta + \phi)$ ; here the angle  $\phi$  accounts for the fact that the island does not necessarily move in the field direction. A complete analysis of stationary island shapes has been achieved in the limiting case of zero stiffness [20]. For an even number  $n$  of symmetry axes smooth stationary shapes are found for small  $S$ , while for larger anisotropy the shapes develop self-intersections; no stationary shapes exist when  $n$  is odd. The migration direction generally lies between the field direction and the symmetry axis of the anisotropy.

Despite their mathematical interest, these results are of limited applicability to real islands, because all stationary shapes are wildly unstable when  $\tilde{\gamma} = 0$ . In the remainder of the article we therefore focus on the numerical solution of the full, time-dependent problem with  $\tilde{\gamma} > 0$  and  $\sigma(\theta)$  given by (2). Two complementary numerical algorithms have been employed. For relatively small islands a finite difference scheme described in [11] was found to be most efficient, while for large islands we rely on the better stability properties of a semi-implicit adaptive finite element algorithm [22]. The full mutual consistency of the two approaches has been checked.

Most results have been obtained for  $n = 6$  and  $\alpha = 0$ . This leaves the anisotropy strength  $S$  and the initial condition for the deterministic shape evolution to be specified. Extensive calculations show that the dependence on the precise initial shape is minor [23], and hence the initial condition can be characterized by the radius  $R_0$  of a circular island of the same area; in practice, we usually start the calculation from a slightly distorted circle.

The phase diagram in Fig.1 gives an overview of the observed migration modes in the  $S - R_0$ -plane [24]. For small islands ( $R_0 \leq 2$ ) the evolution converges to a stationary shape which moves in the direction of the field. For large  $S$  the shapes develop facets [20], similar to what has been observed for void electromigration [11]. Increasing the island radius the direction of migration starts to deviate from the field direction, and we enter the regime of oblique stationary (**os**) motion (Fig.2). Since the field is aligned with the symmetry axis of the anisotropy, the appearance of obliquely moving solutions implies that the

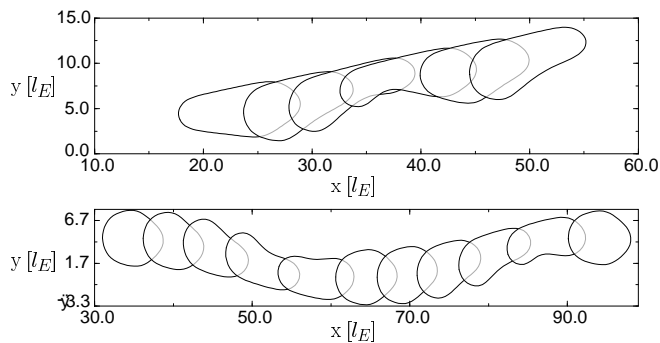


FIG. 3: Snapshots of **oo** motion for  $R_0 = 4$  and  $S = 1$  (upper panel) and **zz** motion for  $R_0 = 3.5$ ,  $S = 0.5$  (lower panel), taken at time intervals  $\Delta t = 20$ . In both cases the perimeter displays simple oscillations, as in the bottom panel of Fig.4.

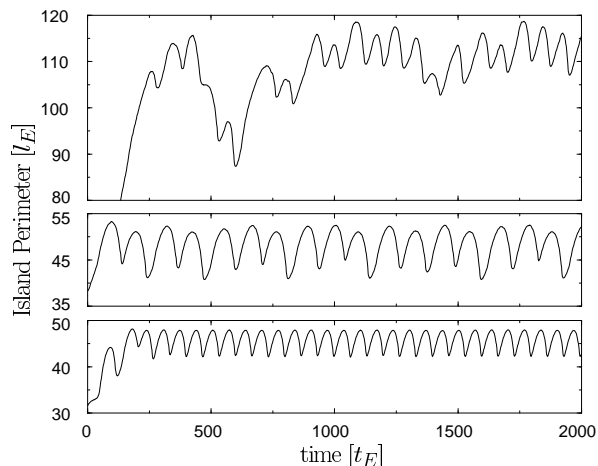


FIG. 4: Time series of the island perimeter showing regular and irregular oscillations. From bottom to top the parameters are  $S = 2, R_0 = 5$ ;  $S = 5, R_0 = 5$ ; and  $S = 3, R_0 = 8$ . The top panel corresponds to the run shown in Fig.5.

symmetry of the problem is *spontaneously* broken. In the **os** regime, pairs of symmetry-related stationary solutions coexist; which solution is chosen in a given run depends on the initial condition.

Upon further increase of  $R_0$  the obliquely moving shapes start to oscillate (Fig.3). Near the onset of oblique oscillatory (**oo**) motion at radius  $R_0^c$  the oscillation period diverges as  $T \sim |R_0 - R_0^c|^{-\nu}$  with  $\nu \approx 2.5$ . For larger radii higher harmonics of the fundamental oscillation period appear and the motion becomes increasingly irregular (Fig.4). This characterizes the complex oscillatory (**co**) regime, which is exemplified in Fig.5. The direction of island motion displays random shifts, which seem to be triggered by small fluctuations. This behavior is typical for large islands, and it is distinct from the *periodic* direction changes seen in the zig-zag (**zz**) regime for moderate sizes and small anisotropies (Fig.3).

The true long time behavior for large islands ( $R_0 > 7$ ) and large anisotropy ( $S > 5$ ) could not be pinned down

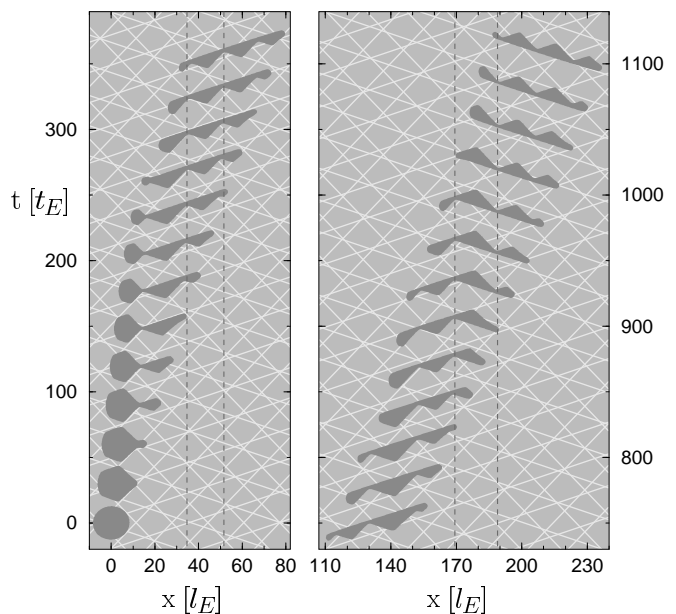


FIG. 5: Complex oscillatory motion with  $S = 3$ ,  $R_0 = 8$ . Light lines show the facet orientations predicted from (3), dark dashed lines illustrate that the hill-valley structure is static in the substrate frame. Consecutive snapshots are shifted upwards in time.

unambiguously with our current numerical methods. Generally speaking, large islands with small anisotropy break up, while for large  $R_0$  and  $S$  faceted shapes undergoing irregular motion dominate.

The example shown in Fig.5 provides an important clue to the origin of the complex shape evolution. After an initial transient lasting until  $t \approx 300$ , the island settles down into a shape consisting of a straight upper edge and a lower edge which has broken up into a faceted hill-and-valley structure. The direction of island motion coincides with the orientation of the upper, straight edge, as shown for a smaller island in the upper panel of Fig.3. The key observation is that the hill-and-valley structure on the faceted edge *does not move* in the substrate frame. The moving island slides past the static facets, causing the shape to oscillate. Around  $t \approx 900$  the roles of the upper and lower edges are seen to reverse, and the direction of motion changes.

Quite generally, large islands in the **co** regime can be constructed from four selected facet orientations  $\theta_1, \theta_2, \theta_3, \theta_4$ . Here  $\theta_1$  and  $\theta_2$  are the possible stable orientations of the upper island edge, which must satisfy  $-\pi/2 < \theta_1 < 0 < \theta_2 < \pi/2$ . In the case considered here ( $\alpha = 0$ ,  $n$  even) the corresponding orientations  $\theta_3$  and  $\theta_4$  for the lower edge are obtained by reflection at the  $x$ -axis,  $\theta_3 = -\pi - \theta_1$  and  $\theta_4 = \pi - \theta_2$ . To form a closed shape, at least three orientations must be combined, two of which are those two symmetry-related orientations that are closest to the horizontal direction ( $\theta = 0$  or  $\pi$ ). In Fig.5 we see a transition from a shape with orientations

$\{\theta_1, \theta_3, \theta_4\}$  to a shape with orientations  $\{\theta_1, \theta_2, \theta_3\}$ .

The stable facet orientations can be computed along the lines of [25]. The condition  $v_n = 0$  for a static shape implies that the current in (1) is set to a constant  $j^*$ . Using the relation  $\kappa = d\theta/ds$  this can be brought into the form

$$\Omega\tilde{\gamma}\frac{d^2}{ds^2}\theta = -[j^*/\sigma(\theta) - q^*E_0\cos(\theta)] \equiv -V'(\theta), \quad (3)$$

which describes the position  $\theta(s)$  of a particle moving in time  $s$  subject to a potential  $V(\theta)$  determined by the mobility and the electric field strength. As explained in [25], the coexistence of two stable facet orientations corresponds to a particle trajectory moving between two degenerate potential maxima. To determine the selected orientations,  $j^*$  is tuned until two degenerate maxima satisfying the above constraints appear. We have checked that this procedure correctly accounts for the facet orientations observed in the time-dependent calculations throughout the relevant region of the phase diagram (see Fig.5). In general, stable facets can be constructed from (3) only when the anisotropy is sufficiently large [25]. For  $n = 6$ ,  $\alpha = 0$  the requirement is  $S > S_c \approx 1.77$ . No stable facets are found when the number of symmetry axes is too small ( $n \leq 3$ ); this may explain why we do not see oscillatory shape evolution for a threefold anisotropy.

Shapes similar to those in Fig.5 have been seen previously in the nonlocal model of void electromigration, but there breakup usually takes place soon after the hill-valley structure has developed (see Fig. 11 of [11]). This seems to be caused by the deepening of the valleys between the transiently stable facets, which is related to a tendency to develop overhangs in the nonlocal case [26].

From the perspective of nonlinear dynamics, it is interesting to note that the observed island shapes are quite smooth, which implies that the number of circular harmonics involved in the shape evolution is small. It thus seems promising to attempt a description in terms of a low-dimensional dynamical system, in the spirit of [14], to gain a deeper understanding of the various migration modes and the bifurcations connecting them.

It remains to address the experimental conditions under which the predictions of this paper could be realized. As an example, we consider islands on Cu(100), for which most material parameters entering the theory are available. Following [5], we estimate that the electromigration force on an edge atom at a current density of  $10^7 \text{ Acm}^{-2}$  is about 400 eV/cm. Together with the experimentally determined stiffness [15] and mobility [16] for kinked steps at 300 K, this yields a characteristic length of  $l_E \approx 25 \text{ nm}$ , and a time scale  $t_E$  on the order of seconds. Thus we expect complex shape dynamics to be observable for island radii around 100 nm and on time scales of a few hundred seconds. As a first step towards a more detailed description of specific surfaces, it would

be important to identify oscillatory shape evolution in kinetic Monte Carlo simulations of island electromigration.

This work was supported by DFG within SFB 616 *Energy dissipation at surfaces* and SFB 611 *Singular phenomena and scaling in mathematical models*.

---

\* krug@thp.uni-koeln.de

- [1] T. Michely, J. Krug, *Islands, Mounds and Atoms. Patterns and Processes in Crystal Growth Far from Equilibrium*. (Springer, Berlin 2004).
- [2] K. Yagi, H. Minoda, M. Degawa, Surf. Sci. Rep. **43**, 45 (2001).
- [3] J.-J. Métois, J.-C. Heyraud, A. Pimpinelli, Surf. Sci. **420**, 250 (1999).
- [4] A. Saúl, J.-J. Métois, A. Ranguis, Phys. Rev. B **65**, 075409 (2002).
- [5] H. Mehl, O. Biham, O. Millo, M. Karimi, Phys. Rev. B **61**, 4975 (2000).
- [6] O. Pierre-Louis, T.L. Einstein, Phys. Rev. B **62**, 13697 (2000).
- [7] S. V. Khare, N. C. Bartelt, T. L. Einstein, Phys. Rev. Lett. **75**, 2148 (1995).
- [8] D.-J. Liu, J.W. Evans, Phys. Rev. B **66**, 165407 (2002).
- [9] W.W. Pai *et al.*, Phys. Rev. Lett. **86**, 3088 (2001)
- [10] M. Schimschak, J. Krug, Phys. Rev. Lett. **80**, 1674 (1998).
- [11] M. Schimschak, J. Krug, J. Appl. Phys. **87**, 685 (2000).
- [12] M.R. Gungor, D. Maroudas, Surf. Sci. **461**, L550 (2000).
- [13] K. Kassner, C. Misbah, H. Müller-Krumbhaar, Phys. Rev. Lett. **67**, 1551 (1991).
- [14] A. Valance, K. Kassner, C. Misbah, Phys. Rev. Lett. **69**, 1544 (1992).
- [15] S. Dieluweit, H. Ibach, M. Giesen, T.L. Einstein, Phys. Rev. B **67**, 121410 (2003).
- [16] M. Giesen, S. Dieluweit, J. Mol. Cat. A **216**, 263 (2004).
- [17] Z. Suo, W. Wang, M. Yang, Appl. Phys. Lett. **64** 1944 (1994).
- [18] W. Yang, W. Wang, Z. Suo, J. Mech. Phys. Solids **42** 897 (1994).
- [19] W. Wang, Z. Suo, T.-H.Hao, J. Appl. Phys. **79**, 2394 (1996).
- [20] P. Kuhn, J. Krug, in *Multiscale modeling of epitaxial growth*, ed. by A. Voigt (Birkhäuser, in press), cond-mat/0405068.
- [21] Preliminary numerical calculations indicate that the scenarios described here are largely preserved in the presence of an anisotropic stiffness (F. Hausser, unpublished).
- [22] F. Hausser, A. Voigt, in *Multiscale modeling of epitaxial growth*, ed. by A. Voigt (Birkhäuser, in press).
- [23] In some cases, however, an elongated initial shape can be stabilized for island sizes where a more circular initial condition leads to breakup.
- [24] Similar migration modes have been observed for  $n = 4$  and for  $n = 6$  with other values of  $\alpha$ , with the exception of the case  $n = 6$  and  $\alpha = \pi/6$ , where only straight moving stationary states are observed.
- [25] J. Krug, H.T. Dobbs, Phys. Rev. Lett. **73**, 1947 (1994).
- [26] M. Schimschak, J. Krug, Phys. Rev. Lett. **78**, 278 (1997).